Closed-Form Dynamic Model of Planar Multilink Lightweight Robots

Alessandro De Luca, *Member, IEEE*, and Bruno Siciliano, *Member, IEEE*

Abstract—**Closed-form equations of motion are presented for planar lightweight robot arms with multiple flexible links. The kinematic model is based on standard frame transformation matrices describing both rigid rotation and flexible displacement, under small deflection assumption. The Lagrangian approach is used to derive the dynamic model of the structure. Links are modeled as Euler–Bernoulli beams with proper clamped-mass boundary conditions. The assumed modes method is adopted in order to obtain a finite-dimensional model. Explicit equations of motion are detailed for a two-link case assuming two modes of vibration for each link. The associated eigenvalue problem is discussed in relation with the problem of time-varying mass boundary conditions for the first link. The model is cast in a compact form that is linear with respect to a suitable set of constant parameters. Extensive simulation results are included that validate the theoretical derivation.**

I. Introduction

LIGHTWEIGHT MECHANICAL STRUCTURES are expected to improve performance of robot manipulators with typically low payload-to-arm weight ratio. The ultimate goal of such robotic designs is to achieve fast and dexterous motion as opposed to slow and bulky motion of conventional industrial robots. Although the transfer to applications of advanced research findings in this field is still in its infancy, we believe that the realization of effective lightweight robots may prove very promising in a number of innovative areas including manipulation with very long arms, teleoperation, and space robotics.

In order to fully exploit the potential advantages offered by lightweight robot arms, one must explicitly consider the effects of structural link flexibility and properly deal with (active and/or passive) control of vibrational behavior. In this context, it is highly desirable to have an *explicit*, *complete*, *accurate* dynamic model at disposal. The model should be *explicit* to provide a clear understanding of dynamic interaction and coupling effects, to be useful for control design, and to guide reduction and/or simplification based on terms relevance. The model should be *complete* in that it is simple enough (e.g., finite- versus infinite-dimensional) while inheriting the most relevant properties; viz., many of the explicit models were developed for one-link flexible arms, not showing the full nonlinear aspects of the general case. The model should be *accurate* as required by advanced model-based nonlinear controllers (e.g., inversion techniques [1], output regulation [2], adaptive control [3]) and by off-line optimal trajectory generation [4].

The techniques employed for modeling open serial kinematic chains containing one or more flexible members adopt the same formulations as in the case of rigid links, i.e., Newton–Euler, Lagrange–Euler, and Kane. All of them are based on a suitable kinematic description of both rigid and deflected motions.

As for the inherently distributed character of the flexible part of the system, finite-dimensional models are required in order to approximate the "true" infinite-dimensional model [5]. In any case, link elasticity is usually characterized as a *linear* effect. The most used approximate descriptions of the deflection are based on assumed modes [6], [7], finite elements [8], [9], or Ritz–Kantorovich expansions [10], with different implications on model complexity and accuracy.

On one hand, explicit models have been derived for the case of a one-link flexible arm [6], [7], [11], [12]. In this regard, it can be said that the one-link case is now well understood, but its simplicity prevents from thoroughly understanding the full nonlinear interactions between rigid and flexible components of arm dynamics.

On the other hand, various formalisms have been proposed for dynamic modeling of multilink flexible arms [13]–[15]. To cope with the computational burden of the general case, symbolic manipulation languages prove helpful for automatic model generation [16]–[18]. Besides, a number of numerical software packages have been developed for simulation purposes [19], [20]. One intrinsic limitation of resorting to general purpose techniques and/or programs, however, is that the resulting model is either only *implicitly* specified or presented in a poorly structured form. In any case, the control engineer is offered scarce insight into the origin of the single dynamic terms.

The aim of this work is to derive a dynamic model of multilink flexible robot arms, limiting ourselves to the case of planar manipulators with no torsional effects. The main emphasis is on obtaining a customized model that satisfies the aforementioned requirements about explicitness, completeness, and accuracy. As a result, we can arrange the equations of motion in a computationally efficient closed form that is also *linear* with respect to a suitable set of constant mechanical parameters.

In particular, the model is derived adopting the Lagrangian

Manuscript received August 11, 1990; revised February 16, 1991. This paper is based on work supported by Ministero dell'Università e della Ricerca Scientifica e Tecnologica under 60% funds and partly by Consiglio Nazionale delle Ricerche under contract no. 90.00381.PF67.

A. De Luca is with the Dipartimento di Informatica e Sistemistica Università degli Studi di Roma "La Sapienza" Via Eudossiana 18, 00184 Roma, Italy.

B. Siciliano is with the Dipartimento di Informatica e Sistemistica Università degli Studi di Napoli "Federico II" Via Claudio 21, 80125 Napoli, Italy

IEEE Log Number 9144659.

0018–9472/91$01.00 © 1991 IEEE

technique in conjunction with the assumed modes method. Links are modeled as Euler–Bernoulli beams satisfying proper clamped-mass boundary conditions. A payload is added at the tip of the outer link, while hub inertias are included at the actuated joints.

As a case study, a two-link arm is considered using two modes of bending deformation for each link. It is argued that this case is general enough to provide a basis for analyzing more complex structures, since most of the possible dynamic interaction effects are present. Preliminary results can be found in [21], [22]. In this framework are also the contributions reported in [23]–[26]. Further, we investigate the implications of having time-varying mass boundary conditions for the eigenvalue problem associated with the first link. A set of simulation results are provided to validate the overall modeling in forward dynamics.

We would like to remark that for the case of spatial manipulators, including torsional and coupled deformation effects, derivation of closed-form dynamic models is much more complex and requires use of symbolic manipulation programs. Therefore, extensions to three-dimensional cases are not pursued here since they are believed to go beyond the present desire of obtaining a complete, explicit, well-understood model.

The paper is organized as follows: Section II gives the kinematic description in a recursive form for planar multilink flexible arms. The typical steps involved in the Lagrangian method are presented in Section III, i.e., derivation of kinetic and potential energy. Section IV is devoted to the modeling of link deflection by means of assumed mode shapes with proper boundary conditions. The closed-form equations of motion are assembled in Section V. The explicit dynamic model for the two-link flexible arm is given in Section VI, with the expressions of model coefficients detailed in Appendix. Section VII reports simulation results for the system, both in free and forced evolution. Conclusions are drawn in the final section.

II. Kinematic Modeling

Consider a planar n-link flexible arm with rotary joints subject only to bending deformations in the plane of motion (torsional effects are neglected); Fig. 1 shows a two-link example. According to [13], the following coordinate frames are established: the inertial frame $(\widehat{X}_0, \widehat{Y}_0)$, the rigid body moving frame associated to link i (X_i, Y_i), and the flexible body moving frame associated to link i $(\widehat{X}_i, \widehat{Y}_i)$. The rigid motion is described by the joint angles θ_i, while $y_i(x_i)$ denotes the transversal deflection of link i at abscissa x_i, $0 \leq x_i \leq \ell_i$, being ℓ_i the link length.

Let ${}^i\boldsymbol{p}_i(x_i) = (x_i \; y_i(x_i))^{\mathrm{T}}$ be the position of a point along the deflected link i with respect to frame (X_i, Y_i) and $\boldsymbol{p}_i$ be the absolute position of the same point in frame $(\widehat{X}_0, \widehat{Y}_0)$. Also, ${}^i\boldsymbol{r}_{i+1} = {}^i\boldsymbol{p}_i(\ell_i)$ indicates the position of the origin of frame (X_{i+1}, Y_{i+1}) with respect to frame (X_i, Y_i), and $\boldsymbol{r}_i$ its absolute position in frame $(\widehat{X}_0, \widehat{Y}_0)$.

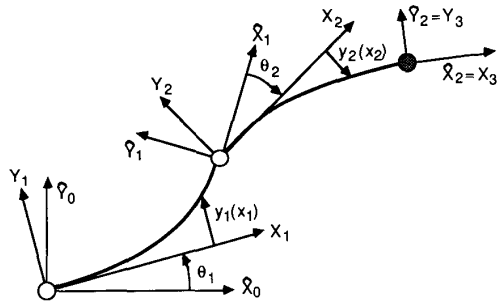

Fig. 1. A planar two-link flexible arm.

The joint (rigid) rotation matrix $\boldsymbol{A}_i$ and the rotation matrix $\boldsymbol{E}_i$ of the (flexible) link at the end-point are, respectively,

$$\boldsymbol{A}_i = \begin{bmatrix} \cos\theta_i & -\sin\theta_i \\ \sin\theta_i & \cos\theta_i \end{bmatrix}, \qquad \boldsymbol{E}_i = \begin{bmatrix} 1 & -y'_{ie} \\ y'_{ie} & 1 \end{bmatrix}, \quad (1)$$

where $y'_{ie} = (\partial y_i/\partial x_i)|_{x_i=\ell_i}$, and the linear approximation $\arctan y'_{ie} \simeq y'_{ie}$, valid for small deflections, has been made. This also implies that all second-order terms involving products of deformations are neglected. Therefore, the previous absolute position vectors can be expressed as

$$\boldsymbol{p}_i = \boldsymbol{r}_i + \boldsymbol{W}_i {}^i\boldsymbol{p}_i, \qquad \boldsymbol{r}_{i+1} = \boldsymbol{r}_i + \boldsymbol{W}_i {}^i\boldsymbol{r}_{i+1} \quad (2)$$

where $\boldsymbol{W}_i$ is the global transformation matrix from $(\widehat{X}_0, \widehat{Y}_0)$ to (X_i, Y_i), which obeys to the recursive equation

$$\boldsymbol{W}_i = \boldsymbol{W}_{i-1}\boldsymbol{E}_{i-1}\boldsymbol{A}_i = \widehat{\boldsymbol{W}}_{i-1}\boldsymbol{A}_i, \qquad \widehat{\boldsymbol{W}}_0 = \boldsymbol{I}. \quad (3)$$

On the basis of the previous relations, the kinematics of any point along the arm is fully characterized.

For later use in the arm's kinetic energy, also the differential kinematics is needed. In particular, the (scalar) absolute angular velocity of frame (X_i, Y_i) is

$$\dot{\alpha}_i = \sum_{j=1}^{i} \dot{\theta}_j + \sum_{k=1}^{i-1} \dot{y}'_{ke} \quad (4)$$

where the upper dot denotes time derivative. Moreover, the absolute linear velocity of an arm point is

$$\dot{\boldsymbol{p}}_i = \dot{\boldsymbol{r}}_i + \dot{\boldsymbol{W}}_i {}^i\boldsymbol{p}_i + \boldsymbol{W}_i {}^i\dot{\boldsymbol{p}}_i \quad (5)$$

and ${}^i\dot{\boldsymbol{r}}_{i+1} = {}^i\dot{\boldsymbol{p}}_i(\ell_i)$. Since the links are assumed unextensible ($\dot{x}_i = 0$), then ${}^i\dot{\boldsymbol{p}}_i(x_i) = (0 \; \dot{y}_i(x_i))^{\mathrm{T}}$. The computation of (5) takes advantage of the recursions

$$\dot{\boldsymbol{W}}_i = \dot{\widehat{\boldsymbol{W}}}_{i-1}\boldsymbol{A}_i + \widehat{\boldsymbol{W}}_{i-1}\dot{\boldsymbol{A}}_i, \qquad \dot{\widehat{\boldsymbol{W}}}_i = \dot{\boldsymbol{W}}_i\boldsymbol{E}_i + \boldsymbol{W}_i\dot{\boldsymbol{E}}_i. \quad (6)$$

Also, note that

$$\dot{\boldsymbol{A}}_i = \boldsymbol{S}\boldsymbol{A}_i\dot{\theta}_i, \qquad \dot{\boldsymbol{E}}_i = \boldsymbol{S}\dot{y}'_{ie}, \qquad \boldsymbol{S} = \begin{bmatrix} 0 & -1 \\ 1 & 0 \end{bmatrix}. \quad (7)$$

III. Lagrangian Modeling

The dynamic equations of motion of a planar n-link flexible arm can be derived following the standard Lagrangian approach, i.e., by computing the kinetic energy T and the potential energy U of the system and then forming the Lagrangian $L = T - U$.

The total kinetic energy is given by the sum of the following contributions:

$$T = \sum_{i=1}^{n} T_{hi} + \sum_{i=1}^{n} T_{\ell i} + T_p. \tag{8}$$

The kinetic energy of the rigid body located at hub i of mass m_{hi} and moment of inertia J_{hi} is

$$T_{hi} = \frac{1}{2} m_{hi} \dot{\boldsymbol{r}}_i^{\mathrm{T}} \dot{\boldsymbol{r}}_i + \frac{1}{2} J_{hi} \dot{\alpha}_i^2 \tag{9}$$

with $\dot{\alpha}_i$ as in (4), the kinetic energy pertaining to link i of linear density ρ_i is

$$T_{\ell i} = \frac{1}{2} \int_0^{\ell_i} \rho_i(x_i) \dot{\boldsymbol{p}}_i^{\mathrm{T}}(x_i) \dot{\boldsymbol{p}}_i(x_i) dx_i, \tag{10}$$

and the kinetic energy associated to a payload of mass m_p and moment of inertia J_p located at the end of link n is

$$T_p = \frac{1}{2} m_p \dot{\boldsymbol{r}}_{n+1}^{\mathrm{T}} \dot{\boldsymbol{r}}_{n+1} + \frac{1}{2} J_p (\dot{\alpha}_n + \dot{y}'_{ne})^2. \tag{11}$$

Remarkably, the evaluation of the expressions in (9)–(11) exploits the following identities:

$$\boldsymbol{A}_i^T \boldsymbol{A}_i = \boldsymbol{E}_i^{\mathrm{T}} \boldsymbol{E}_i = \boldsymbol{S}^{\mathrm{T}} \boldsymbol{S} = \boldsymbol{I}, \tag{12a}$$

$$\boldsymbol{A}_i^T \dot{\boldsymbol{A}}_i = \boldsymbol{S} \dot{\theta}_i, \qquad \boldsymbol{E}_i^{\mathrm{T}} \dot{\boldsymbol{E}}_i = (\boldsymbol{I} y'_{ie} + \boldsymbol{S}) \dot{y}'_{ie}. \tag{12b}$$

In absence of gravity (horizontal plane motion), the potential energy is given by

$$U = \sum_{i=1}^{n} U_i = \sum_{i=1}^{n} \frac{1}{2} \int_0^{\ell_i} (EI)_i(x_i) \left[\frac{d^2 y_i(x_i)}{dx_i^2} \right]^2 dx_i, \tag{13}$$

where U_i is the elastic energy stored in link i, being $(EI)_i$ its flexural rigidity.

Notice that no discretization of structural link flexibility has been made so far. As a result of the aforementioned expressions, the overall Lagrangian will be a *functional*, due to the inherent distributed nature of the dynamical system. This "exact" Lagrangian can be shown to generate an infinite-dimensional model, which is of limited use for simulation and/or control purposes. Therefore, a finite-dimensional representation of link deflection is introduced next.

IV. Assumed Mode Shapes

Links are modeled as Euler–Bernoulli beams of uniform density ρ_i and constant flexural rigidity $(EI)_i$, with deformation $y_i(x_i, t)$ satisfying the partial differential equation

$$(EI)_i \frac{\partial^4 y_i(x_i,t)}{\partial {x_i}^4} + \rho_i \frac{\partial^2 y_i(x_i,t)}{\partial t^2} = 0, \qquad i = 1, \ldots, n. \tag{14}$$

In order to solve this equation, proper boundary conditions have to be imposed at the base and at the end of each link.

It is reasonable to suppose that the inertia of a lightweight link is small compared to the hub inertia, and then constrained mode shapes can be used [11]. In particular, we assume each slewing link to be *clamped* at the base

$$y_i(0,t) = 0, \qquad y_i'(0,t) = 0, \qquad i = 1, \ldots, n. \tag{15}$$

Furthermore, experiments [7] and recent analytical studies [27] have shown that the clamped assumption is even enforced when closing a feedback control loop around the joint.

Concerning the remaining boundary conditions, it is usually assumed that the link end is *free* of dynamic constraints, due to the difficulty of accounting for time-varying or unknown masses and inertias. We argue, however, that it is more correct to consider *mass* boundary conditions representing balance of moment and shearing force, i.e.,

$$\begin{aligned}
(EI)_i \frac{\partial^2 y_i(x_i,t)}{\partial {x_i}^2}\bigg|_{x_i=\ell_i} &= -J_{Li} \frac{d^2}{dt^2} \left(\frac{\partial y_i(x_i,t)}{\partial x_i}\bigg|_{x_i=\ell_i} \right) \\
&\quad - (MD)_i \frac{d^2}{dt^2} (y_i(x_i,t)|_{x_i=\ell_i}) \\
(EI)_i \frac{\partial^3 y_i(x_i,t)}{\partial {x_i}^3}\bigg|_{x_i=\ell_i} &= M_{Li} \frac{d^2}{dt^2} (y_i(x_i,t)|_{x_i=\ell_i}) \\
&\quad + (MD)_i \frac{d^2}{dt^2} \left(\frac{\partial y_i(x_i,t)}{\partial x_i}\bigg|_{x_i=\ell_i} \right) \\
&\quad i = 1, \ldots, n,
\end{aligned} \tag{16}$$

where M_{Li} and J_{Li} are the *actual* mass and moment of inertia at the end of link i. Moreover, $(MD)_i$ accounts for the contributions of masses of distal links, i.e., noncollocated at the end of link i, weighted by the relative distance from axis $\widehat{Y}_i$ (shearing axis at the end of link i). Incidentally, these contributions are often not included in mode shape analyses.

A finite-dimensional model (of order m_i) of link flexibility can be obtained by the assumed modes technique [5]. Exploiting separability in time and space of solutions to (14), the link deflection can be expressed as

$$y_i(x_i,t) = \sum_{j=1}^{m_i} \phi_{ij}(x_i) \delta_{ij}(t) \tag{17}$$

where $\delta_{ij}(t)$ are the time-varying variables associated with the assumed spatial mode shapes $\phi_{ij}(x_i)$ of link i. Therefore, each term in the general solution to (14) is the product of a time harmonic function of the form

$$\delta_{ij}(t) = \exp(j\omega_{ij} t) \tag{18}$$

and of a space eigenfunction of the form

$$\begin{aligned}
\phi_{ij}(x_i) = &C_{1,ij} \sin(\beta_{ij} x_i) + C_{2,ij} \cos(\beta_{ij} x_i) + C_{3,ij} \sinh(\beta_{ij} x_i) \\
&+ C_{4,ij} \cosh(\beta_{ij} x_i).
\end{aligned} \tag{19}$$

In (18), ω_{ij} is the jth natural angular frequency of the eigenvalue problem for link i, and in (19), $\beta_{ij}^4 = \omega_{ij}^2 \rho_i / (EI)_i$.

Application of the aforementioned boundary conditions allows the determination of the constant coefficients in (19). The clamped conditions at the link base yield

$$C_{3,ij} = -C_{1,ij}, \qquad C_{4,ij} = -C_{2,ij} \tag{20}$$

while the mass conditions at the link end lead to a homogeneous system of the form

$$\left[\boldsymbol{F}(\beta_{ij})\right]\begin{bmatrix} C_{1,ij} \\ C_{2,ij} \end{bmatrix} = \boldsymbol{0}. \tag{21}$$

The so-called frequency equation is obtained by setting to zero the determinant of the (2×2) matrix $\boldsymbol{F}(\beta_{ij})$ that depends explicitly on the values M_{Li}, J_{Li}, and $(MD)_i$ [25]. The first m_i roots of this equation give the positive values β_{ij} (and thus ω_{ij}) to be plugged in (19). Using these values, the coefficients $C_{1,ij}$ and $C_{2,ij}$ are determined up to a scale factor that is chosen via a suitable normalization. Further, the resulting eigenfunctions ϕ_{ij} satisfy a modified orthogonality condition that includes the actual M_{Li}, J_{Li}, and $(MD)_i$.

Notice that, if the arm has only one link, M_{L1} and J_{L1} are directly the payload mass and inertia, while the additional terms on the right-hand side of (16) vanish ($(MD)_1 = 0$) only when the payload is balanced at the tip. For the generic intermediate ith link in an open kinematic chain arrangement, instead, M_{Li} is the *constant* sum of all masses beyond link i, but J_{Li} and $(MD)_i$ *depend* on the position of successive links. Thus, for exact mode shapes computation, these quantities should be updated as functions of the arm configuration; this may considerably increase the complexity of model derivation, beside overloading the computational burden of on-line execution [16]. Therefore, some practical approximation leading to constant—although nonzero—boundary conditions at the link end might be in order.

For instance, a convenient position is to set $(MD)_i = 0$ and compute J_{Li} for a fixed arm configuration. In this case, it can be shown that $\det(\boldsymbol{F}) = 0$ results into the transcendental equation [1]:

$$\begin{aligned}
&\Big(1 + \cos(\beta_{ij}\ell_i)\cosh(\beta_{ij}\ell_i)\Big) \\
&- \frac{M_{Li}\beta_{ij}}{\rho_i}\Big(\sin(\beta_{ij}\ell_i)\cosh(\beta_{ij}\ell_i) - \cos(\beta_{ij}\ell_i)\sinh(\beta_{ij}\ell_i)\Big) \\
&- \frac{J_{Li}{\beta_{ij}}^3}{\rho_i}\Big(\sin(\beta_{ij}\ell_i)\cosh(\beta_{ij}\ell_i) + \cos(\beta_{ij}\ell_i)\sinh(\beta_{ij}\ell_i)\Big) \\
&+ \frac{M_{Li}J_{Li}{\beta_{ij}}^4}{\rho_i^2}\Big(1 - \cos(\beta_{ij}\ell_i)\cosh(\beta_{ij}\ell_i)\Big) = 0.
\end{aligned} \tag{22}$$

The two-link case study worked out in Section VI will provide further insight into the problem of nonconstant boundary conditions.

V. Closed-Form Equations of Motion

On the basis of the discretization introduced in the previous section, the Lagrangian L becomes a function of a set of N generalized coordinates $\{q_i(t)\}$, and the dynamic model is obtained by satisfying the Lagrange–Euler equations

$$\frac{d}{dt}\frac{\partial L}{\partial \dot{q}_i} - \frac{\partial L}{\partial q_i} = f_i, \qquad i = 1, \ldots, N, \tag{23}$$

where $\{f_i\}$ are the generalized forces performing work on $\{q_i\}$.

Under the assumption of constant mode shapes, it can be shown that the spatial dependence present in the link kinetic energy term (10) can be resolved by the introduction of a number of constant parameters, characterizing the mechanical properties of the (uniform density) links [17], [28]:

$$m_i = \int_0^{\ell_i} \rho_i dx_i = \rho_i \ell_i, \tag{24a}$$

$$d_i = \frac{1}{m_i}\int_0^{\ell_i} \rho_i x_i dx_i = \frac{1}{2}\ell_i, \tag{24b}$$

$$J_{oi} = \int_0^{\ell_i} \rho_i {x_i}^2 dx_i = \frac{1}{3} m_i {\ell_i}^2, \tag{24c}$$

$$v_{ij} = \int_0^{\ell_i} \rho_i \phi_{ij}(x_i) dx_i, \tag{24d}$$

$$w_{ij} = \int_0^{\ell_i} \rho_i \phi_{ij}(x_i) x_i dx_i, \tag{24e}$$

$$z_{ijk} = \int_0^{\ell_i} \rho_i \phi_{ij}(x_i)\phi_{ik}(x_i) dx_i, \tag{24f}$$

$$k_{ijk} = \int_0^{\ell_i} (EI)_i \phi_{ij}(x_i)\phi_{ik}(x_i) dx_i. \tag{24g}$$

Therefore, m_i is the mass of link i, d_i is the distance of center of mass of link i from joint i axis, J_{oi} is the inertia of link i about joint i axis, v_{ij} and w_{ij} are deformation moments of order zero and one of mode j of link i, and z_{ijk} is the cross moment of modes j and k of link i. Also, k_{ijk} is the cross elasticity coefficient of modes j and k of link i. The actual numerical values of the previous parameters can be computed off-line. Existing CAD packages, which are available for solid modeling, conveniently serve this purpose for more complex link shapes.

As a result of this procedure, the equations of motion for a planar n-link flexible arm can be written in the familiar closed form

$$\boldsymbol{B}(\boldsymbol{q})\ddot{\boldsymbol{q}} + \boldsymbol{h}(\boldsymbol{q}, \dot{\boldsymbol{q}}) + \boldsymbol{K}\boldsymbol{q} = \boldsymbol{Q}\boldsymbol{u} \tag{25}$$

where $\boldsymbol{q} = (\theta_1 \ldots \theta_n \delta_{11} \ldots \delta_{1,m_1} \ \ldots \ \delta_{n,1} \ldots \delta_{n,m_n})^{\mathrm{T}}$ is the N-vector of generalized coordinates ($N = n + \sum_i m_i$), and $\boldsymbol{u}$ is the n-vector of joint (actuator) torques. $\boldsymbol{B}$ is the positive-definite symmetric inertia matrix, $\boldsymbol{h}$ is the vector of Coriolis and centrifugal forces, $\boldsymbol{K}$ is the stiffness matrix, and $\boldsymbol{Q}$ is the input weighting matrix that is of the form $[\boldsymbol{I}_{n\times n}\, \boldsymbol{O}_{n\times(N-n)}]^{\mathrm{T}}$ due to the clamped link assumption. If desired, joint viscous friction and link structural damping can be added as $\boldsymbol{D}\dot{\boldsymbol{q}}$, where $\boldsymbol{D}$ is a diagonal matrix.

It should be remarked that orthonormalization of mode shapes implies convenient simplifications in the diagonal blocks of the inertia matrix relative to the deflections of each link, due to the particular values attained by z_{ijk} in (24f). Also,

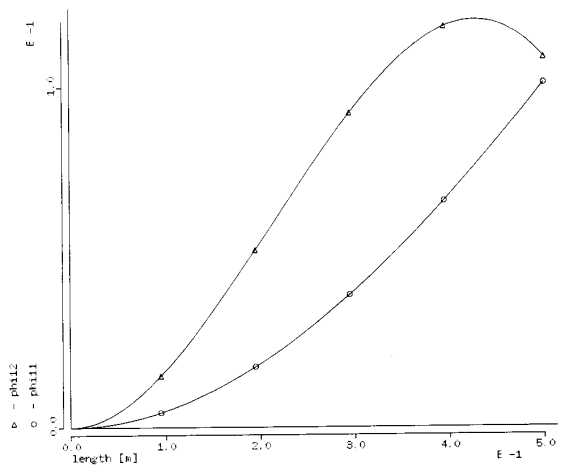

(a)

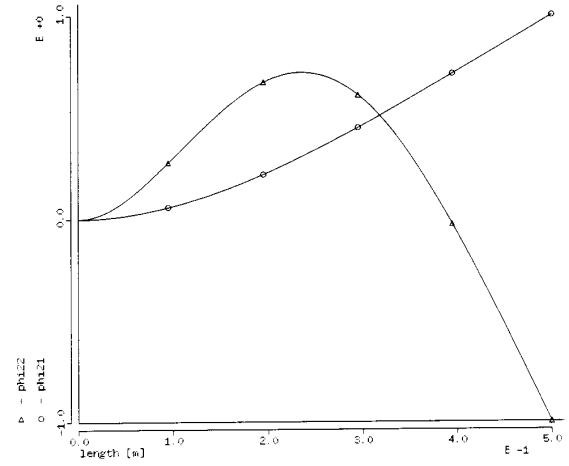

(b)

Fig. 2. (a) Mode shapes for link 1 (no payload). (b) Mode shapes for link 2 (no payload)

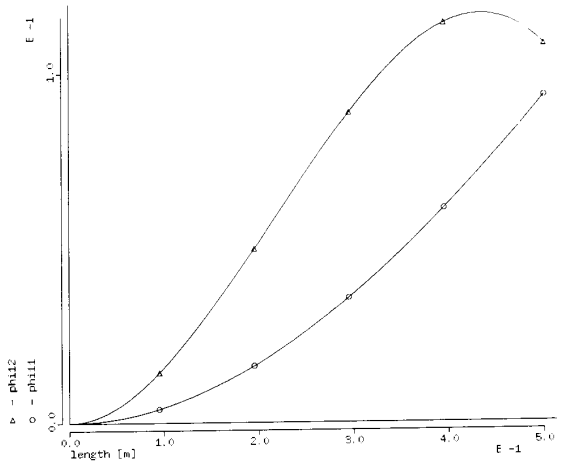

(a)

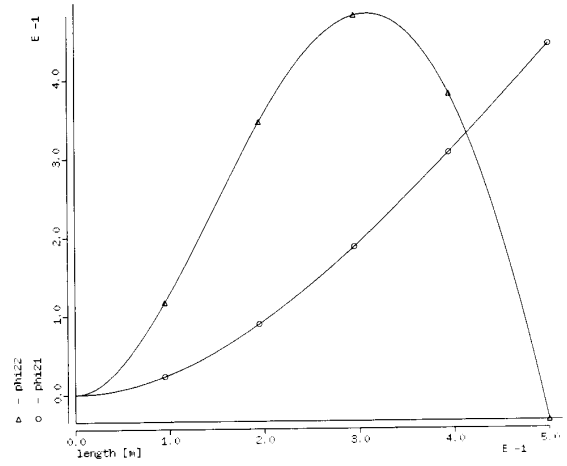

(b)

Fig. 3. (a) Mode shapes for link 1 (nominal payload). (b) Mode shapes for link 2 (nominal payload).

the stiffness matrix becomes diagonal ($K_1 = \ldots = K_n = 0; K_{n+1}, \ldots, K_N > 0$) being $k_{ijk} = 0$ for $j \neq k$ in (24g).

Regarding the components of $\boldsymbol{h}$, these can be evaluated through the Christoffel symbols, i.e.,

$$h_i = \sum_{j=1}^{N}\sum_{k=1}^{N}\left(\frac{\partial B_{ij}}{\partial q_k} - \frac{1}{2}\frac{\partial B_{jk}}{\partial q_i}\right)\dot{q}_j\dot{q}_k. \tag{26}$$

VI. Explicit Dynamic Model of a Two-Link Flexible Arm

We present now the explicit finite-dimensional dynamic model of a two-link flexible arm ($n = 2$) with two assumed mode shapes for each link ($m_1 = m_2 = 2$). Thus, the vector of Lagrangian coordinates reduces to $\boldsymbol{q} = (\theta_1\theta_2\delta_{11}\delta_{12}\delta_{21}\delta_{22})^{\mathrm{T}}$, i.e., $N = 6$. This reduced order model is sufficient to encompass the relevant flexibility issues occurring in practical experimental control of lightweight manipulators, with limited bandwidth actuators.

As pointed out in the previous sections, the process of mode shapes orthonormalization is of great importance for model simplification. In this case, it can be shown that the contributions to kinetic energy due to deflection variables are

$$\{\text{factor of } \dot{\delta}_{i1}^2\} = z_{i11}, \tag{27a}$$

$$\{\text{factor of } 2\dot{\delta}_{i1}\dot{\delta}_{i2}\} = \begin{bmatrix}\phi_{i1,e} & \phi'_{i1,e}\end{bmatrix} \cdot \begin{bmatrix} M_{Li} & \frac{1}{2}(MD)_i \\ \frac{1}{2}(MD)_i & J_{Li}\end{bmatrix}\begin{bmatrix}\phi_{i2,e} \\ \phi'_{i2,e}\end{bmatrix} + z_{i12}, \tag{27b}$$

$$\{\text{factor of } \dot{\delta}_{i2}^2)\} = z_{i22}, \tag{27c}$$

where $\phi_{ij,e} = \phi_{ij}(x_i)|_{x_i=\ell_i}$ and $\phi'_{ij,e} = \phi'_{ij}(x_i)|_{x_i=\ell_i}$, $i, j = 1, 2$. Equations (27a)–(27c) are obtained expanding terms (10) and (11) by using (4) and (5). Accounting for separability (17) then leads to expressions for the factors of the quadratic deflection rate terms, in which the parameters defined in (24f) and the mass coefficients on the right-hand side of (16) can

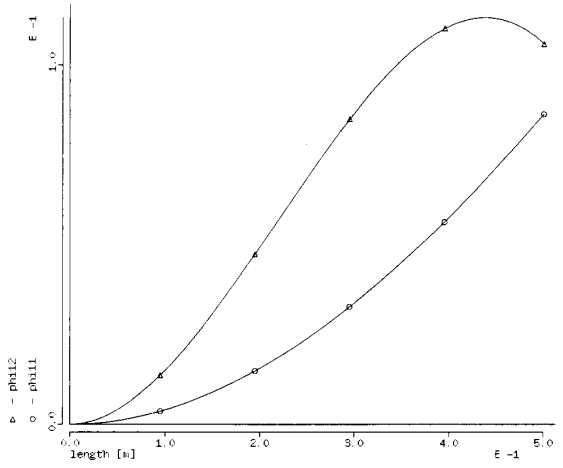

(a)

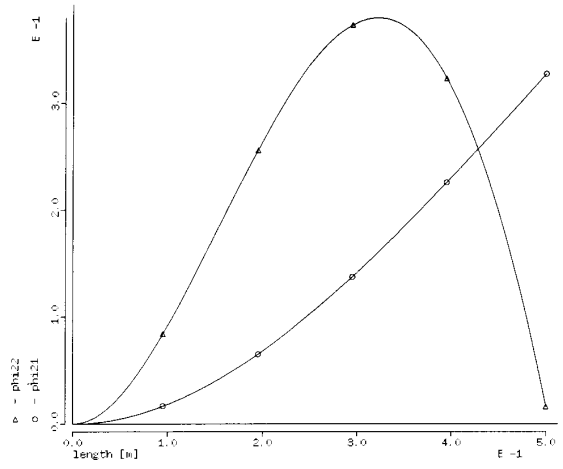

(b)

Fig. 4. (a) Mode shapes for link 1 (double payload). (b) Mode shapes for link 2 (double payload).

be identified. It is found that for link 1:

$$\begin{aligned} M_{L1} &= m_2 + m_{h2} + m_p \\ J_{L1} &= J_{o2} + J_{h2} + J_p + m_p \ell_2^2, \end{aligned} \tag{28}$$

$$\begin{aligned} (MD)_1 =& (m_2 d_2 + m_p \ell_2) \cos\theta_2 - [(v_{21} + m_p \phi_{21,e})\delta_{21} \\ &+ (v_{22} + m_p \phi_{22,e})\delta_{22}] \sin\theta_2. \end{aligned}$$

Notice that in the considered case of only two links, J_{L1} is a constant. For more than two links, J_{L1} will become a function of the generalized coordinates of link 3 and following ones. On the other hand, for link 2:

$$M_{L2} = m_p, \qquad J_{L2} = J_p, \qquad (MD)_2 = 0. \tag{29}$$

A convenient normalization of mode shapes is accomplished by setting:

$$z_{ijj} = m_i, \qquad i, j = 1, 2. \tag{30}$$

This also implies that the nonzero coefficients in the stiffness matrix $\boldsymbol{K}$ take on the values $\omega_{ij}^2 m_i$. We stress that, if the exact values for the boundary conditions in (16) (i.e., the expressions provided by (28) and (29)) were used, the natural orthogonality of the computed mode shapes would imply that {factor of $2\dot{\delta}_{i1}\dot{\delta}_{i2}$} is zero for both links.

Regarding link 2, use of (29) automatically ensures the "correct" orthogonality of mode shapes. On the other hand, the issue is more critical for link 1 because of the off-diagonal term $(MD)_1$, which varies with the arm configuration. This implies that the mode shapes—which are *spatial* quantities—would become implicit functions of *time*, thus conflicting with the original *separability* assumption (!). In particular, it can be seen that when the second link is stretched out ($\theta_2 = 0$), $(MD)_1$ reduces to $m_2 d_2 + m_p \ell_2$. When the second link is at a right angle with the first ($\theta_2 = \pm\pi/2$), $(MD)_1$ becomes $\mp[(v_{21} + m_p \phi_{21,e})\delta_{21} + (v_{22} + m_p \phi_{22,e})\delta_{22}]$, so that the actual mode shapes of the first link become themselves functions of the time-varying variables describing the deflection of the second link.

A common approximation in computing the elements of the inertia matrix for flexible structures is to evaluate kinetic energy in correspondence to the undeformed configuration. In our case, this is equivalent to neglecting the second term of $(MD)_1$ in (28), which is an order of magnitude smaller than the first term. Accordingly, $(MD)_1$ can be rendered constant for a fixed arm configuration. In particular, taking $\theta_2 = \pm\pi/2$ leads to $(MD)_1 = 0$, and thus eigenfrequencies can be computed through (22). This is equivalent to having zeroed only that portion of {factor of $2\dot{\delta}_{11}\dot{\delta}_{12}$} generated by the constant diagonal terms, i.e.,

$$[\phi_{11,e}, \phi'_{11,e}] \begin{bmatrix} M_{L1} & 0 \\ 0 & J_{L1} \end{bmatrix} \begin{bmatrix} \phi_{12,e} \\ \phi'_{12,e} \end{bmatrix} + z_{112} = 0. \tag{31}$$

This will be seen to produce nonzero off-diagonal terms in the relative block of the inertia matrix.

The resulting model is cast in a computationally advantageous form, where a set of constant coefficients appear that depend on the mechanical parameters of the arm.

The inertia matrix turns out of the form

$$\begin{aligned} B_{11} &= b_{111} + b_{112}c_2 + (b_{113}t_1 + b_{114}t_2)s_2 \\ B_{12} &= b_{121} + b_{122}c_2 + (b_{123}t_1 + b_{124}t_2)s_2 \\ B_{13} &= b_{131} + b_{132}c_2 + (b_{133}t_2 + b_{134}\delta_{12})s_2 \\ B_{14} &= b_{141} + b_{142}c_2 + (b_{143}t_2 + b_{144}\delta_{11})s_2 \\ B_{15} &= b_{151} + b_{152}c_2 + b_{153}t_1 s_2 \\ B_{16} &= b_{161} + b_{162}c_2 + b_{163}t_1 s_2 \end{aligned} \tag{32a}$$

$$\begin{aligned} B_{22} &= b_{221} \\ B_{23} &= b_{231} + b_{232}c_2 + (b_{233}t_2 + b_{234}t_3)s_2 \\ B_{24} &= b_{241} + b_{242}c_2 + (b_{243}t_2 + b_{244}t_3)s_2 \\ B_{25} &= b_{251} \\ B_{26} &= b_{261} \end{aligned} \tag{32b}$$

$$B_{33} = b_{331} + b_{332}c_2 + b_{333}t_2 s_2 \tag{32c}$$

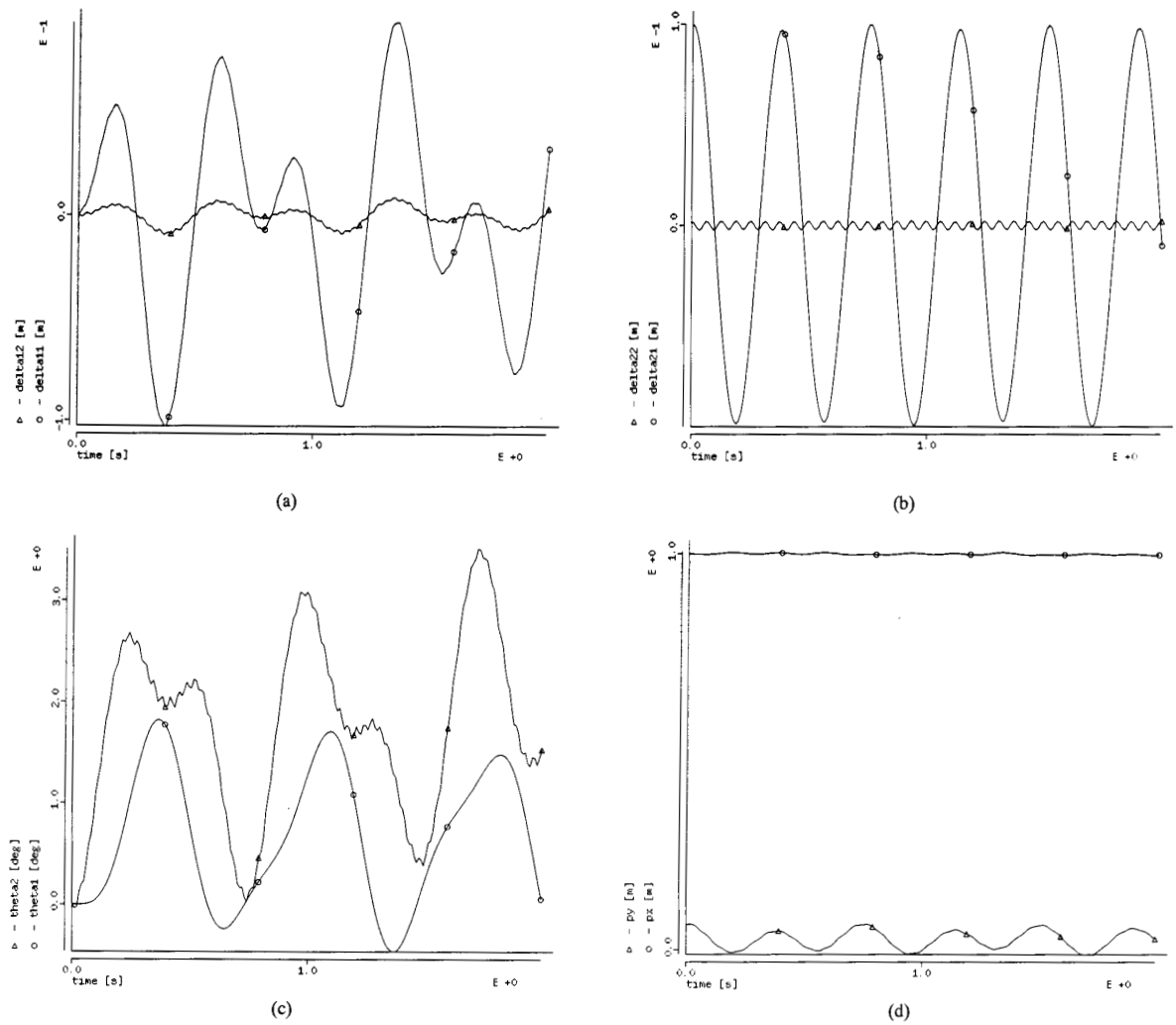

Fig. 5. (a) Deflections of link 1 ($\theta_2(0) = 0$, $\delta_{21}(0) = 0.1$, $\delta_{22}(0) = 0.002$) (b) Deflections of link 2 ($\theta_2(0) = 0$, $\delta_{21}(0) = 0.1$, $\delta_{22}(0) = 0.002$) (c) Joint evolution ($\theta_2(0) = 0$, $\delta_{21}(0) = 0.1$, $\delta_{22}(0) = 0.002$) (d) Tip evolution ($\theta_2(0) = 0$, $\delta_{21}(0) = 0.1$, $\delta_{22}(0) = 0.002$)

$$B_{34} = b_{341} + b_{342}c_2 + b_{343}t_2 s_2$$
$$B_{35} = b_{351} + b_{352}c_2 + b_{353}t_3 s_2$$
$$B_{36} = b_{361} + b_{362}c_2 + b_{363}t_3 s_2$$

$$B_{44} = b_{441} + b_{442}c_2 + b_{443}t_2 s_2 \quad (32d)$$
$$B_{45} = b_{451} + b_{452}c_2 + b_{453}t_3 s_2$$
$$B_{46} = b_{461} + b_{462}c_2 + b_{463}t_3 s_2$$

$$B_{55} = b_{551} \quad (32e)$$
$$B_{56} = b_{561}$$

$$B_{66} = b_{661} \quad (32f)$$

where $s_2 = \sin\theta_2$, $c_2 = \cos\theta_2$, and

$$t_1 = t_{11}\delta_{11} + t_{12}\delta_{12}$$
$$t_2 = t_{21}\delta_{21} + t_{22}\delta_{22}$$
$$t_3 = t_{31}\delta_{11} + t_{32}\delta_{12} \quad (33)$$

with the coefficients having the expressions reported in Appendix. Note that the contributions of deflections to system inertia, i.e., terms containing t_i and δ_{1j}, always appear multiplied by s_2; this derives from the initial assumption on deformation being purely transversal to link axis.

Having obtained the expression of the inertia matrix, the components of $\boldsymbol{h}$ can be evaluated using (26):

$$h_1 = \big[(h_{101}\dot{\theta}_2 + h_{102}\dot{\delta}_{11} + h_{103}\dot{\delta}_{12} + h_{104}\dot{\delta}_{21} + h_{105}\dot{\delta}_{22})\dot{\theta}_1 + (h_{106}\dot{\theta}_2 + h_{107}\dot{\delta}_{11} + h_{108}\dot{\delta}_{12} + h_{109}\dot{\delta}_{21} + h_{110}\dot{\delta}_{22})\dot{\theta}_2 + (h_{111}\dot{\delta}_{21} + h_{112}\dot{\delta}_{22})\dot{\delta}_{11} + (h_{113}\dot{\delta}_{21} + h_{114}\dot{\delta}_{22})\dot{\delta}_{12}\big] s_2$$

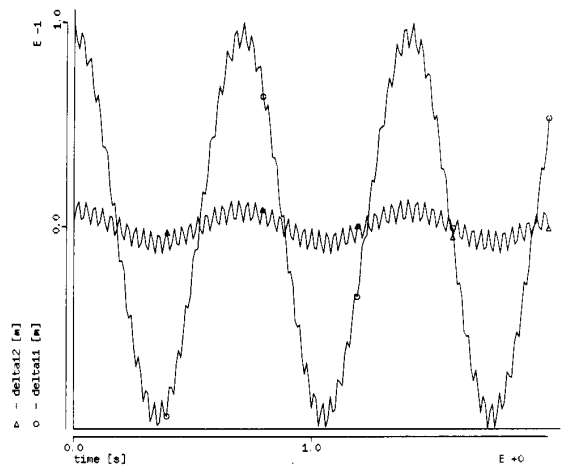

(a)

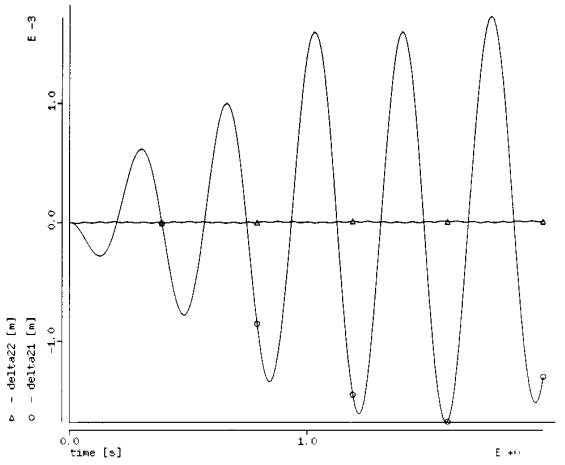

(b)

Fig. 6. (a) Deflections of link 1 ($\theta_2(0) = \pi/2$, $\delta_{11}(0) = 0.1$, $\delta_{12}(0) = 0.002$). (b) Deflections of link 2 ($\theta_2(0) = \pi/2$, $\delta_{11}(0) = 0.1$, $\delta_{12}(0) = 0.002$)

$$+ \left[(h_{115}\dot\theta_1 + h_{116}\dot\theta_2 + h_{117}\dot\delta_{21} + h_{118}\dot\delta_{22})t_1 + (h_{119}\dot\theta_1 + h_{120}\dot\theta_2 + h_{121}\dot\delta_{11} + h_{122}\dot\delta_{12})t_2 + h_{123}\delta_{12}\dot\delta_{11} + h_{124}\delta_{11}\dot\delta_{12}\right]\dot\theta_2 c_2 \quad (34a)$$

$$h_2 = (h_{201}\dot\theta_1 + h_{202}\dot\delta_{11} + h_{203}\dot\delta_{12})\dot\theta_1 s_2 + \Big\{\left[(h_{204}\dot\theta_1 + h_{205}\dot\delta_{21} + h_{206}\dot\delta_{22})t_1 + (h_{207}\dot\theta_1 + h_{208}\dot\delta_{11} + h_{209}\dot\delta_{12})t_2 + h_{210}\delta_{12}\dot\delta_{11} + h_{211}\delta_{11}\dot\delta_{12}\right]\dot\theta_1 + \left[(h_{212}\dot\delta_{11} + h_{213}\dot\delta_{12})t_2 + (h_{214}\dot\delta_{21} + h_{215}\dot\delta_{22})t_3\right]\dot\delta_{11} + \left[h_{216}\dot\delta_{12}t_2 + (h_{217}\dot\delta_{21} + h_{218}\dot\delta_{22})t_3\right]\dot\delta_{12}\Big\}c_2 \quad (34b)$$

$$h_3 = \left[(h_{301}\dot\theta_1 + h_{302}\dot\theta_2 + h_{303}\dot\delta_{12} + h_{304}\dot\delta_{21} + h_{305}\dot\delta_{22})\dot\theta_1 + (h_{306}\dot\theta_2 + h_{307}\dot\delta_{11} + h_{308}\dot\delta_{12} + h_{309}\dot\delta_{21} + h_{310}\dot\delta_{22})\dot\theta_2 + (h_{311}\dot\delta_{21} + h_{312}\dot\delta_{22})\dot\delta_{11} + (h_{313}\dot\delta_{21} + h_{314}\dot\delta_{22})\dot\delta_{12}\right]s_2 + \left[(h_{315}\dot\theta_1 + h_{316}\dot\theta_2 + h_{317}\dot\delta_{11} + h_{318}\dot\delta_{12})t_2 + (h_{319}\dot\theta_2 + h_{320}\dot\delta_{21} + h_{321}\dot\delta_{22})t_3 + h_{322}\delta_{12}\dot\theta_1\right]\dot\theta_2 c_2 \quad (34c)$$

$$h_4 = \left[(h_{401}\dot\theta_1 + h_{402}\dot\theta_2 + h_{403}\dot\delta_{11} + h_{404}\dot\delta_{21} + h_{405}\dot\delta_{22})\dot\theta_1 + (h_{406}\dot\theta_2 + h_{407}\dot\delta_{11} + h_{408}\dot\delta_{12} + h_{409}\dot\delta_{21} + h_{410}\dot\delta_{22})\dot\theta_2 + (h_{411}\dot\delta_{21} + h_{412}\dot\delta_{22})\dot\delta_{11} + (h_{413}\dot\delta_{21} + h_{414}\dot\delta_{22})\dot\delta_{12}\right]s_2 + \left[(h_{415}\dot\theta_1 + h_{416}\dot\theta_2 + h_{417}\dot\delta_{11} + h_{418}\dot\delta_{12})t_2 + (h_{419}\dot\theta_2 + h_{420}\dot\delta_{21} + h_{421}\dot\delta_{22})t_3 + h_{422}\delta_{11}\dot\theta_1\right]\dot\theta_2 c_2 \quad (34d)$$

$$h_5 = (h_{501}\dot\theta_1 + h_{502}\dot\delta_{11} + h_{503}\dot\delta_{12})\dot\theta_1 s_2 + \left[h_{504}t_1\dot\theta_1 + (h_{505}\dot\delta_{11} + h_{506}\dot\delta_{12})t_3\right]\dot\theta_2 c_2 \quad (34e)$$

$$h_6 = (h_{601}\dot\theta_1 + h_{602}\dot\delta_{11} + h_{603}\dot\delta_{12})\dot\theta_1 s_2 + \left[h_{604}t_1\dot\theta_1 + (h_{605}\dot\delta_{11} + h_{606}\dot\delta_{12})t_3\right]\dot\theta_2 c_2 \quad (34f)$$

with the coefficients having the expressions reported in Appendix.

Finally, the stiffness matrix $\boldsymbol{K}$ is of the form

$$\boldsymbol{K} = \text{diag}\{0,\ 0,\ \omega_{11}^2 m_1,\ \omega_{12}^2 m_1,\ \omega_{21}^2 m_2,\ \omega_{22}^2 m_2\}. \quad (35)$$

VII. Simulation Results

In order to test the dynamic model equations, a two-link flexible arm with the following physical parameters has been considered:

$\rho_1 = \rho_2 = 0.2$ kg/m (uniform density),
$\ell_1 = \ell_2 = 0.5$ m, $d_2 = 0.25$ m,
$m_1 = m_2 = m_p = 0.1$ kg, $m_{h2} = 1$ kg,
$J_{o1} = J_{o2} = 0.0083$ kg m^2,
$J_{h1} = J_{h2} = 0.1$ kg m^2,
$J_p = 0.0005$ kg m^2, and
$(EI)_1 = (EI)_2 = 1$ N m^2.

Different payload conditions have been selected for modal analysis, namely zero, nominal and double payload. Figs. 2–4 show the resulting mode shapes, with the y-axis scaled by the link length. It can be recognized that a variation in the tip payload, though changing the boundary values M_{L1} and J_{L1} (see (28)), does not substantially modify the shapes of link 1 (Figs. 2(a), 3(a), 4(a)). Conversely, the effect of payload on mode shapes of link 2 is evident (Figs. 2(b), 3(b), 4(b)). In particular, the usual node at $x_2 > 0$ in ϕ_{22} of the clamped-free case [5] moves rightwards with increasing payloads, up to disappearing for a sufficiently heavy one.

In the following, we pursue only the nominal payload condition. In this case, the natural frequencies $f_{ij} = \omega_{ij}/2\pi$ are

$f_{11} = 0.48$ Hz, $f_{12} = 1.80$ Hz;
$f_{21} = 2.18$ Hz, $f_{22} = 15.91$ Hz.

Further, the remaining parameters appearing in the model coefficients are computed:

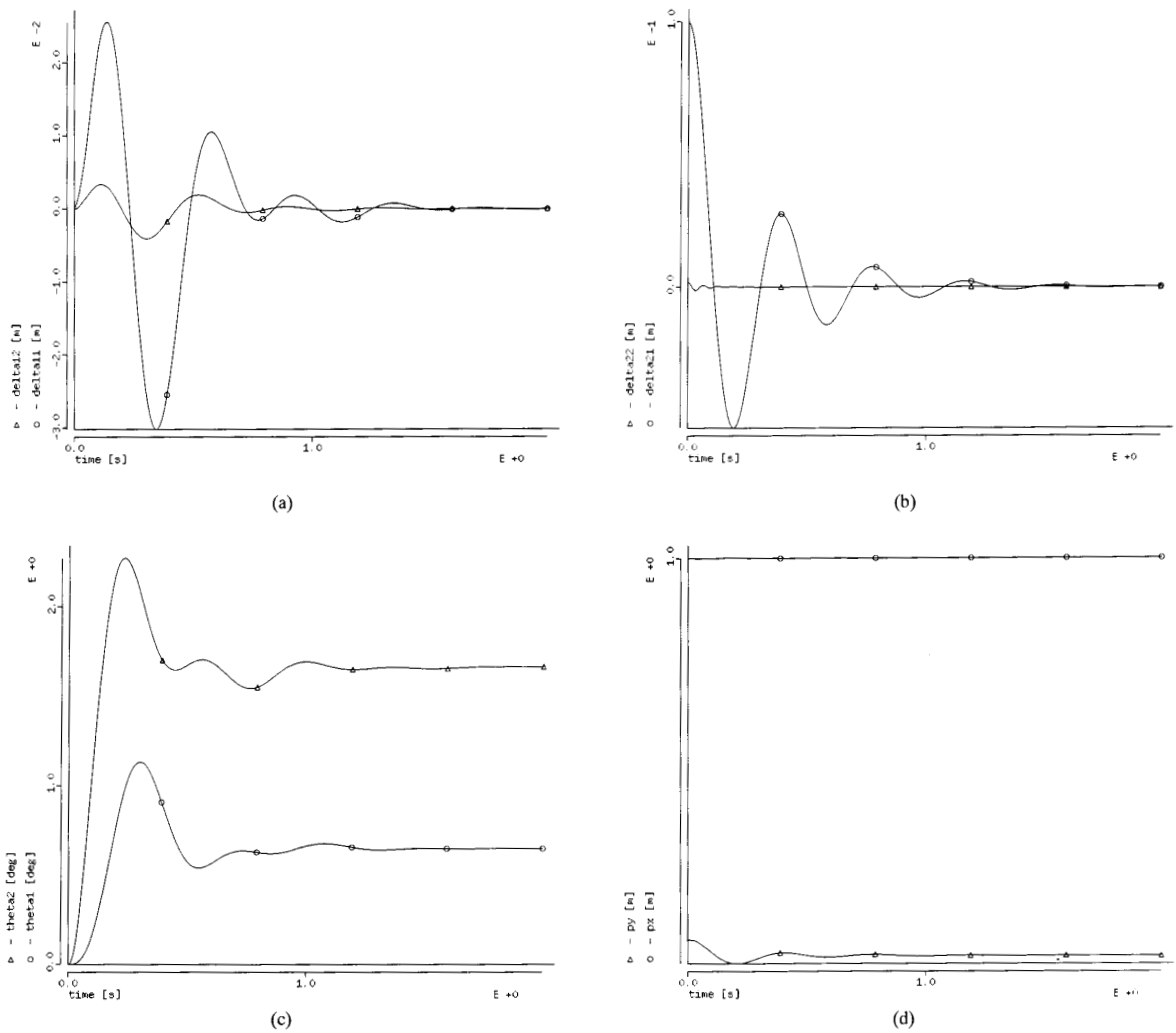

Fig. 7. (a) Deflections of link 1 with damping ($\theta_2(0) = 0$, $\delta_{21}(0) = 0.1$, $\delta_{22}(0) = 0.002$). (b) Deflections of link 2 with damping ($\theta_2(0) = 0$, $\delta_{21}(0) = 0.1$, $\delta_{22}(0) = 0.002$). (c) Joint evolution with damping ($\theta_2(0) = 0$, $\delta_{21}(0) = 0.1$, $\delta_{22}(0) = 0.002$). (d) Tip evolution with damping ($\theta_2(0) = 0$, $\delta_{21}(0) = 0.1$, $\delta_{22}(0) = 0.002$)

$\phi_{11,e} = 0.186$, $\phi_{12,e} = 0.215$,
$\phi'_{11,e} = 0.657$, $\phi'_{12,e} = -0.560$;
$\phi_{21,e} = 0.883$, $\phi_{22,e} = -0.069$,
$\phi'_{21,e} = 2.641$, $\phi'_{22,e} = -10.853$;
$v_{11} = 0.007$, $v_{12} = 0.013$;
$v_{21} = 0.033$, $v_{22} = 0.054$;
$w_{11} = 0.002$, $w_{12} = 0.004$;
$w_{21} = 0.012$, $w_{22} = 0.016$.

A set of numerical simulations have been performed to validate the theoretical model, both in free and in forced evolution. The nonlinear equations of motions have been integrated via a fourth order Runge-Kutta method, and simulations run for 2 sec at 1 msec integration step.

Figs. 5–8 show the dependence of the internal vibrations of the arm on the joint configuration when an initial deformation is given to the system. In the first case, the arm is fully extended ($\theta_2(0) = 0$) and a deformation is imposed to link 2 ($\delta_{21}(0) = 0.1$, $\delta_{22}(0) = 0.002$); Figs. 5(a) and (b) indicate the presence of a strong vibration coupling between the two links. The associated joint and tip motions are reported in Figs. 5(c) and (d), where a slow relative drifting phenomenon can be observed. In the second case, link 2 is posed at right angle with link 1 ($\theta_2(0) = \pi/2$), and the deformation is on link 1 ($\delta_{11}(0) = 0.1$, $\delta_{12}(0) = 0.002$); the transfer of vibrational energy from upper arm to forearm is limited, as revealed by Figs. 6(a) and (b) (note the two orders of magnitude difference on δ_{2j}).

The addition of passive structural damping ($D_i = 0.1\sqrt{K_i}$, $i = 3, \ldots, 6$) provides uniform improvement in the arm motion for both the previous initial configurations, as evidenced in Figs. 7 and 8; this time, the initial displacement results into a net bias in the final arm position.

Next, a symmetric bang-bang input torque of 0.2 N m has been applied at both joints starting from $\theta_1(0) = \theta_2(0) = 0$.

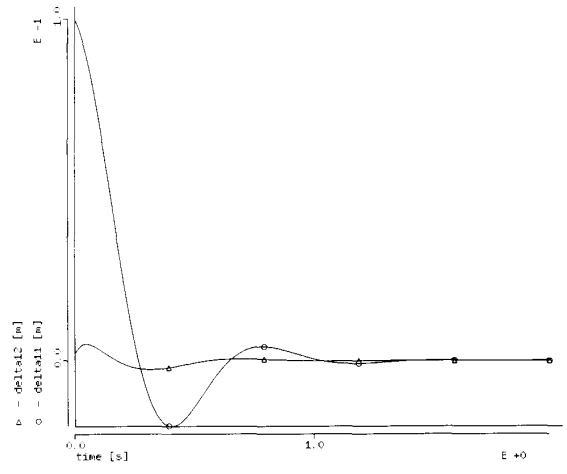

(a)

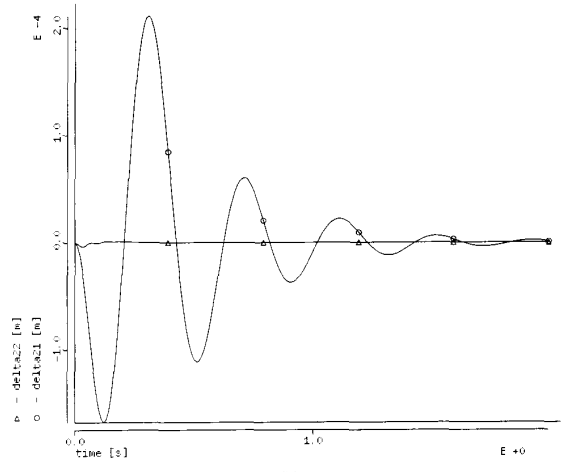

(b)

Fig. 8. (a) Deflections of link 1 with damping ($\theta_2(0) = \pi/2$, $\delta_{11}(0) = 0.1$, $\delta_{12}(0) = 0.002$). (b) Deflections of link 2 with damping ($\theta_2(0) = \pi/2$, $\delta_{11}(0) = 0.1$, $\delta_{12}(0) = 0.002$)

As one could expect, this induces large and coupled vibrations on both links (Figs. 9(a) and (b)), which are reflected in the oscillations at both the joint (Fig. 9(c)) and the tip (Fig. 9(d)) level. This behavior is smoothed down with the introduction of damping (Fig. 10).

VIII. Conclusion

A closed-form finite-dimensional dynamic model for planar multilink lightweight robots has been derived using the Lagrangian approach combined with the assumed modes method. The emphasis has been set on obtaining accurate and complete equations of motion that display the most relevant aspects of the coupling between rigid and flexible dynamics. In particular, the implications of a detailed mode shape analysis on model simplification have been exploited. The crucial problem of time-varying mass boundary conditions has been discussed with reference to a two-link arm, considering two modes of vibration for each link. An explicit nonlinear model has been presented that is cast in an attractive compact form that is linear with respect to a suitable set of constant parameters. Incidentally, this linearity property mimicks the rigid link case and can easily be generalized to any number of modes. The theoretical model has been tested in simulation study, under free and forced time evolution. Besides, the benefits achievable by the addition of passive damping in the structure have been shown clearly.

Our future research efforts will be devoted to developing model-based nonlinear controllers for this class of flexible arms, especially using inversion techniques aimed at achieving end-effector trajectory tracking. Nonetheless, we believe that the availability of the presented model is of great help for designing other types of controllers as well as for evaluating the performance of different lightweight mechanical constructions by means of a reliable simulation testbed.

Appendix

The expressions of the constant coefficients appearing in matrix $\boldsymbol{B}$ of the two-link flexible arm model (32) are

$$
\begin{aligned}
b_{111} &= J_{h1} + J_{o1} + J_{h2} + m_{h2}\ell_1^2 \\
&\quad + J_{o2} + m_2\ell_1^2 + J_p + m_p(\ell_1^2 + \ell_2^2) \\
b_{112} &= 2(m_2 d_2 + m_p \ell_2)\ell_1 \\
b_{113} &= 2(m_2 d_2 + m_p \ell_2) \\
b_{114} &= -2\ell_1 \\
b_{121} &= J_{h2} + J_{o2} + J_p + m_p \ell_2^2 \\
b_{122} &= (m_2 d_2 + m_p \ell_2)\ell_1 \\
b_{123} &= m_2 d_2 + m_p \ell_2 \\
b_{124} &= -\ell_1 \\
b_{131} &= w_{11} + (J_{h2} + J_{o2} + J_p + m_p \ell_2^2)\phi'_{11,e} \\
&\quad + (m_{h2} + m_2 + m_p)\ell_1 \phi_{11,e} \\
b_{132} &= (m_2 d_2 + m_p \ell_2)(\phi_{11,e} + \ell_1 \phi'_{11,e}) \\
b_{133} &= -(\phi_{11,e} + \ell_1 \phi'_{11,e}) \\
b_{134} &= -(m_2 d_2 + m_p \ell_2)(\phi_{11,e}\phi'_{12,e} - \phi_{12,e}\phi'_{11,e}) \\
b_{141} &= w_{12} + (J_{h2} + J_{o2} + J_p + m_p \ell_2^2)\phi'_{12,e} \\
&\quad + (m_{h2} + m_2 + m_p)\ell_1 \phi_{12,e} \\
b_{142} &= (m_2 d_2 + m_p \ell_2)(\phi_{12,e} + \ell_1 \phi'_{12,e}) \\
b_{143} &= -(\phi_{12,e} + \ell_1 \phi'_{12,e}) \\
b_{144} &= -(m_2 d_2 + m_p \ell_2)(\phi_{12,e}\phi'_{11,e} - \phi_{11,e}\phi'_{12,e}) \\
b_{151} &= w_{21} + J_p \phi'_{21,e} + m_p \ell_2 \phi_{21,e} \\
b_{152} &= (v_{21} + m_p \phi_{21,e})\ell_1 \\
b_{153} &= v_{21} + m_p \phi_{21,e} \\
b_{161} &= w_{22} + J_p \phi'_{22,e} + m_p \ell_2 \phi_{22,e} \\
b_{162} &= (v_{22} + m_p \phi_{22,e})\ell_1 \\
b_{163} &= v_{22} + m_p \phi_{22,e}
\end{aligned}
$$

$$
\begin{aligned}
b_{221} &= J_{h2} + J_{o2} + J_p + m_p \ell_2^2 \\
b_{231} &= (J_{h2} + J_{o2} + J_p + m_p \ell_2^2)\phi'_{11,e} \\
b_{232} &= (m_2 d_2 + m_p \ell_2)\phi_{11,e}
\end{aligned}
$$

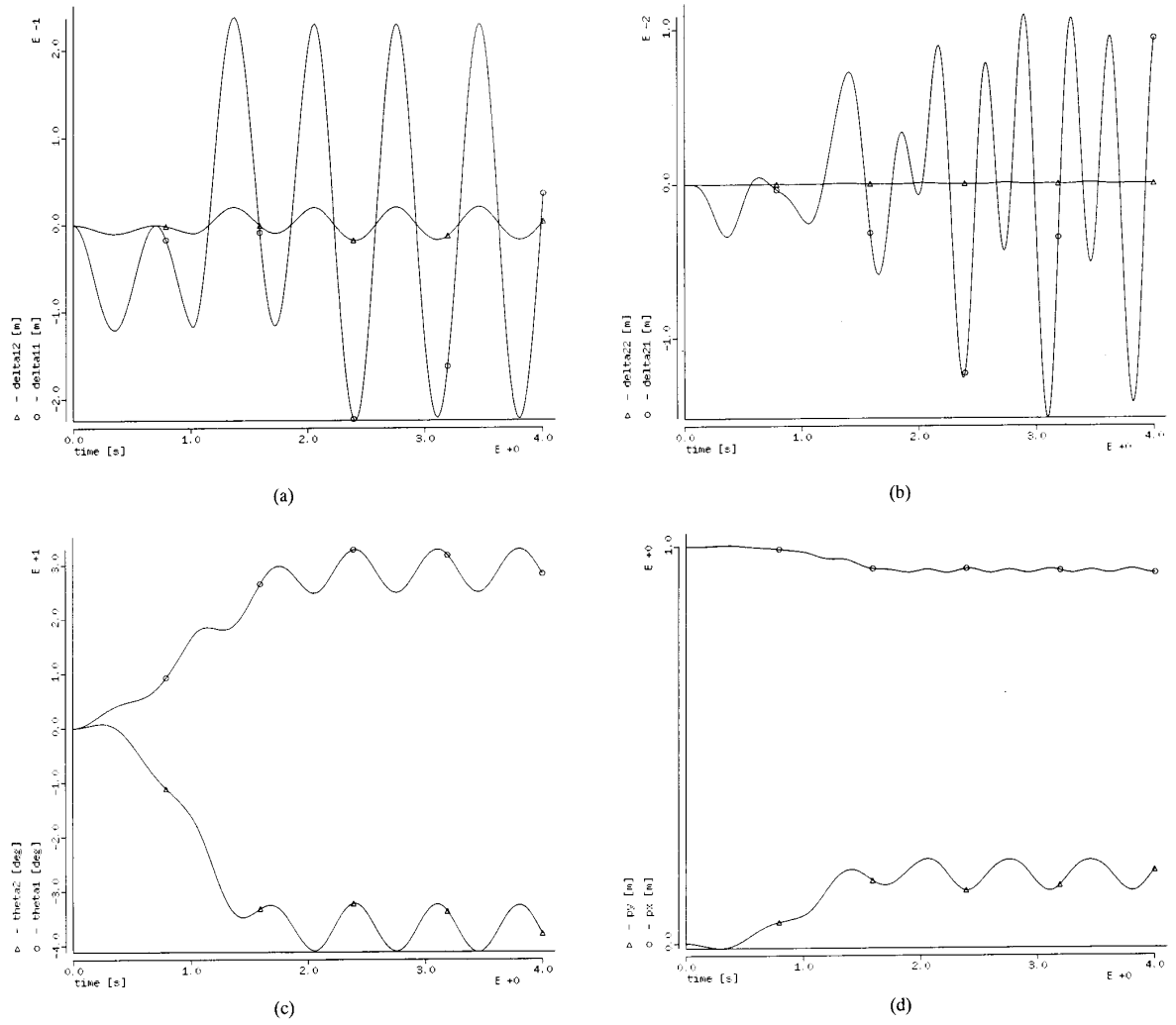

Fig. 9. (a) Deflections of link 1 under bang-bang input ($\theta_1(0) = \theta_2(0) = 0$) (b) Deflections of link 2 under bang-bang input ($\theta_1(0) = \theta_2(0) = 0$) (c) Joint motion under bang-bang input ($\theta_1(0) = \theta_2(0) = 0$) (d) Tip motion under bang-bang input ($\theta_1(0) = \theta_2(0) = 0$)

$$b_{233} = -\phi_{11,e}$$
$$b_{234} = -(m_2 d_2 + m_p \ell_2)\phi_{11,e}$$
$$b_{241} = (J_{h2} + J_{o2} + J_p + m_p \ell_2^2)\phi'_{12,e}$$
$$b_{242} = (m_2 d_2 + m_p \ell_2)\phi_{12,e}$$
$$b_{243} = -\phi_{12,e}$$
$$b_{244} = -(m_2 d_2 + m_p \ell_2)\phi_{12,e}$$
$$b_{251} = w_{21} + J_p \phi'_{21,e} + m_p \ell_2 \phi_{21,e}$$
$$b_{261} = w_{22} + J_p \phi'_{22,e} + m_p \ell_2 \phi_{22,e}$$

$$b_{331} = m_1$$
$$b_{332} = 2(m_2 d_2 + m_p \ell_2)\phi_{11,e}\phi'_{11,e}$$
$$b_{333} = -2\phi_{11,e}\phi'_{11,e}$$
$$b_{341} = 0$$
$$b_{342} = (m_2 d_2 + m_p \ell_2)(\phi_{11,e}\phi'_{12,e} + \phi_{12,e}\phi'_{11,e})$$
$$b_{343} = -(\phi_{11,e}\phi'_{12,e} + \phi_{12,e}\phi'_{11,e})$$
$$b_{351} = (w_{21} + J_p \phi'_{21,e} + m_p \ell_2 \phi_{21,e})\phi'_{11,e}$$
$$b_{352} = (v_{21} + m_p \phi_{21,e})\phi_{11,e}$$
$$b_{353} = -(v_{21} + m_p \phi_{21,e})\phi_{11,e}$$
$$b_{361} = (w_{22} + J_p \phi'_{22,e} + m_p \ell_2 \phi_{22,e})\phi'_{11,e}$$
$$b_{362} = (v_{22} + m_p \phi_{22,e})\phi_{11,e}$$
$$b_{363} = -(v_{22} + m_p \phi_{22,e})\phi_{11,e}$$

$$b_{441} = m_1$$
$$b_{442} = 2(m_2 d_2 + m_p \ell_2)\phi_{12,e}\phi'_{12,e}$$
$$b_{443} = -2\phi_{12,e}\phi'_{12,e}$$
$$b_{451} = (w_{21} + J_p \phi'_{21,e} + m_p \ell_2 \phi_{21,e})\phi'_{12,e}$$
$$b_{452} = (v_{21} + m_p \phi_{21,e})\phi_{12,e}$$
$$b_{453} = -(v_{21} + m_p \phi_{21,e})\phi_{12,e}$$

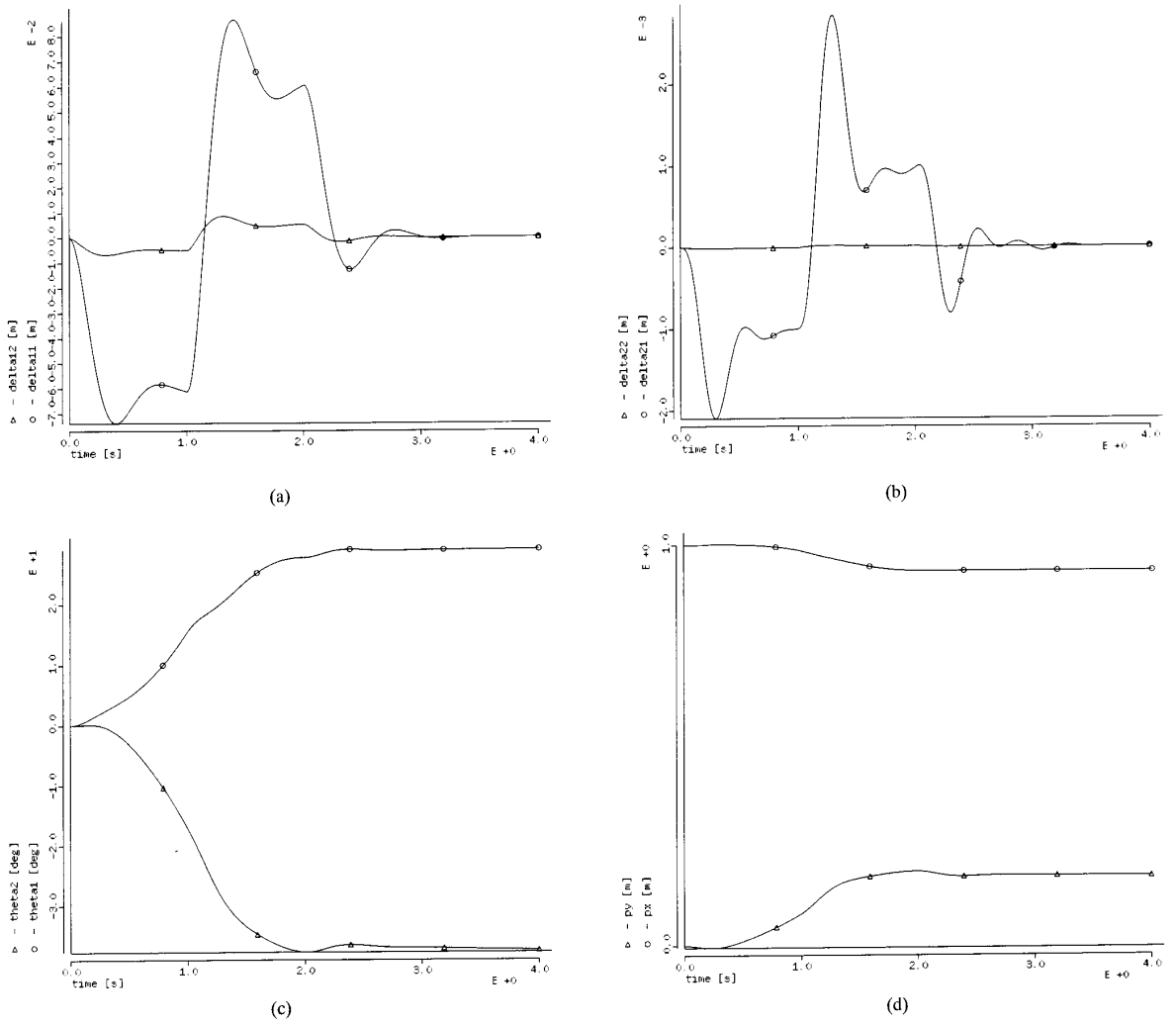

Fig. 10. (a) Deflections of link 1 under bang-bang input with damping ($\theta_1(0) = \theta_2(0) = 0$) (b) Deflections of link 2 under bang-bang input with damping ($\theta_1(0) = \theta_2(0) = 0$) (c) Joint motion under bang-bang input with damping ($\theta_1(0) = \theta_2(0) = 0$) (d) Tip motion under bang-bang input with damping ($\theta_1(0) = \theta_2(0) = 0$)

$$b_{461} = (w_{22} + J_p\phi'_{22,e} + m_p\ell_2\phi_{22,e})\phi'_{12,e}$$
$$b_{462} = (v_{22} + m_p\phi_{22,e})\phi_{12,e}$$
$$b_{463} = -(v_{22} + m_p\phi_{22,e})\phi_{12,e}$$

$$b_{551} = m_2$$
$$b_{561} = 0$$

$$b_{661} = m_2.$$

The terms in the diagonal blocks of $\boldsymbol{B}$ have been simplified by virtue of the orthonormalization procedure described in Section VI. In particular, we have: $b_{551} = b_{661} = m_2$ and $b_{561} = 0$, for the diagonal block relative to link 2 deflections; $b_{331} = b_{441} = m_1$ and $b_{341} = 0$, for the diagonal block relative to link 1 deflections. Due to the choice of *constant* mass boundary conditions for link 1, in the corresponding diagonal block of $\boldsymbol{B}$ nonzero time-varying terms are left that are weighted by coefficients b_{332}, b_{333}, b_{342}, b_{343}, b_{442}, and b_{443}.

The remaining coefficients to be specified in (33) are

$$t_{11} = \phi_{11,e} - \ell_1\phi'_{11,e}$$
$$t_{12} = \phi_{12,e} - \ell_1\phi'_{12,e}$$
$$t_{21} = v_{21} + m_p\phi_{21,e}$$
$$t_{22} = v_{22} + m_p\phi_{22,e}$$
$$t_{31} = \phi'_{11,e}$$
$$t_{32} = \phi'_{12,e}.$$

The expressions of the constant coefficients appearing in vector $\boldsymbol{h}$ of the two-link flexible arm model (34) are

$$h_{101} = -2(m_2d_2 + m_p\ell_2)\ell_1$$
$$h_{102} = 2(m_2d_2 + m_p\ell_2)(\phi_{11,e} - \ell_1\phi'_{11,e})$$

$$h_{103} = 2(m_2d_2 + m_p\ell_2)(\phi_{12,e} - \ell_1\phi'_{12,e})$$
$$h_{104} = -2(v_{21} + m_p\phi_{21,e})\ell_1$$
$$h_{105} = -2(v_{22} + m_p\phi_{22,e})\ell_1$$
$$h_{106} = -(m_2d_2 + m_p\ell_2)\ell_1$$
$$h_{107} = -(m_2d_2 + m_p\ell_2)\ell_1\phi'_{11,e})$$
$$h_{108} = -2(m_2d_2 + m_p\ell_2)\ell_1\phi'_{12,e})$$
$$h_{109} = -2(v_{21} + m_p\phi_{21,e})\ell_1$$
$$h_{110} = -2(v_{22} + m_p\phi_{22,e})\ell_1$$
$$h_{111} = -2(v_{21} + m_p\phi_{21,e})\ell_1\phi'_{11,e}$$
$$h_{112} = -2(v_{22} + m_p\phi_{22,e})\ell_1\phi'_{11,e}$$
$$h_{113} = -2(v_{21} + m_p\phi_{21,e})\ell_1\phi'_{12,e}$$
$$h_{114} = -2(v_{22} + m_p\phi_{22,e})\ell_1\phi'_{12,e}$$
$$h_{115} = 2(m_2d_2 + m_p\ell_2)$$
$$h_{116} = m_2d_2 + m_p\ell_2$$
$$h_{117} = -(v_{21} + m_p\phi_{21,e})$$
$$h_{118} = -(v_{22} + m_p\phi_{22,e})$$
$$h_{119} = -2\ell_1$$
$$h_{120} = -\ell_1$$
$$h_{121} = -(\phi_{11,e} + \ell_1\phi'_{11,e})$$
$$h_{122} = -(\phi_{12,e} + \ell_1\phi'_{12,e})$$
$$h_{123} = -(m_2d_2 + m_p\ell_2)(\phi_{11,e}\phi'_{12,e} - \phi_{12,e}\phi'_{11,e})$$
$$h_{124} = -(m_2d_2 + m_p\ell_2)(\phi_{12,e}\phi'_{11,e} - \phi_{11,e}\phi'_{12,e})$$

$$h_{201} = (m_2d_2 + m_p\ell_2)\ell_1$$
$$h_{202} = 2(m_2d_2 + m_p\ell_2)\phi_{11,e}$$
$$h_{203} = 2(m_2d_2 + m_p\ell_2)\phi_{12,e}$$
$$h_{204} = -(m_2d_2 + m_p\ell_2)$$
$$h_{205} = -(v_{21} + m_p\phi_{21,e})$$
$$h_{206} = -(v_{22} + m_p\phi_{22,e})$$
$$h_{207} = \ell_1$$
$$h_{208} = \phi_{11,e} + \ell_1\phi'_{11,e}$$
$$h_{209} = \phi_{12,e} + \ell_1\phi'_{12,e}$$
$$h_{210} = (m_2d_2 + m_p\ell_2)(\phi_{11,e}\phi'_{12,e} - \phi_{12,e}\phi'_{11,e})$$
$$h_{211} = (m_2d_2 + m_p\ell_2)(\phi_{12,e}\phi'_{11,e} - \phi_{11,e}\phi'_{12,e})$$
$$h_{212} = \phi_{11,e}\phi'_{11,e}$$
$$h_{213} = \phi_{11,e}\phi'_{12,e} + \phi_{12,e}\phi'_{11,e})$$
$$h_{214} = (v_{21} + m_p\phi_{21,e})\phi_{11,e}$$
$$h_{215} = (v_{22} + m_p\phi_{22,e})\phi_{11,e}$$
$$h_{216} = \phi_{12,e}\phi'_{12,e}$$
$$h_{217} = (v_{21} + m_p\phi_{21,e})\phi_{12,e}$$
$$h_{218} = (v_{22} + m_p\phi_{22,e})\phi_{12,e}$$
$$h_{301} = -(m_2d_2 + m_p\ell_2)(\phi_{11,e} - \ell_1\phi'_{11,e})$$
$$h_{302} = -2(m_2d_2 + m_p\ell_2)\phi_{11,e}$$
$$h_{303} = 2(m_2d_2 + m_p\ell_2)(\phi_{12,e}\phi'_{11,e} - \phi_{11,e}\phi'_{12,e})$$
$$h_{304} = -2(v_{21} + m_p\phi_{21,e})\phi_{11,e}$$
$$h_{305} = -2(v_{22} + m_p\phi_{22,e})\phi_{11,e}$$
$$h_{306} = -(m_2d_2 + m_p\ell_2)\phi_{11,e}$$
$$h_{307} = -2(m_2d_2 + m_p\ell_2)\phi_{11,e}\phi'_{11,e}$$
$$h_{308} = -2(m_2d_2 + m_p\ell_2)\phi_{11,e}\phi'_{12,e}$$
$$h_{309} = -2(v_{21} + m_p\phi_{21,e})\phi_{11,e}$$
$$h_{310} = -2(v_{22} + m_p\phi_{22,e})\phi_{11,e}$$
$$h_{311} = -2(v_{21} + m_p\phi_{21,e})\phi_{11,e}\phi'_{11,e}$$
$$h_{312} = -2(v_{22} + m_p\phi_{22,e})\phi_{11,e}\phi'_{11,e}$$
$$h_{313} = -2(v_{21} + m_p\phi_{21,e})\phi_{11,e}\phi'_{12,e}$$
$$h_{314} = -2(v_{22} + m_p\phi_{22,e})\phi_{11,e}\phi'_{12,e}$$
$$h_{315} = -(\phi_{11,e} + \ell_1\phi'_{11,e})$$
$$h_{316} = -\phi_{11,e}$$
$$h_{317} = -2\phi_{11,e}\phi'_{11,e}$$
$$h_{318} = -(\phi_{11,e}\phi'_{12,e} + \phi_{12,e}\phi'_{11,e})$$
$$h_{319} = -(m_2d_2 + m_p\ell_2)\phi_{11,e}$$
$$h_{320} = -(v_{21} + m_p\phi_{21,e})\phi_{11,e}$$
$$h_{321} = -(v_{22} + m_p\phi_{22,e})\phi_{11,e}$$
$$h_{322} = -(m_2d_2 + m_p\ell_2)(\phi_{11,e}\phi'_{12,e} - \phi_{12,e}\phi'_{11,e})$$

$$h_{401} = -(m_2d_2 + m_p\ell_2)(\phi_{12,e} - \ell_1\phi'_{12,e})$$
$$h_{402} = -2(m_2d_2 + m_p\ell_2)\phi_{12,e}$$
$$h_{403} = 2(m_2d_2 + m_p\ell_2)(\phi_{11,e}\phi'_{12,e} - \phi_{12,e}\phi'_{11,e})$$
$$h_{404} = -2(v_{21} + m_p\phi_{21,e})\phi_{12,e}$$
$$h_{405} = -2(v_{22} + m_p\phi_{22,e})\phi_{12,e}$$
$$h_{406} = -(m_2d_2 + m_p\ell_2)\phi_{12,e}$$
$$h_{407} = -2(m_2d_2 + m_p\ell_2)\phi_{12,e}\phi'_{11,e}$$
$$h_{408} = -2(m_2d_2 + m_p\ell_2)\phi_{12,e}\phi'_{12,e}$$
$$h_{409} = -2(v_{21} + m_p\phi_{21,e})\phi_{12,e}$$
$$h_{410} = -2(v_{22} + m_p\phi_{22,e})\phi_{12,e}$$
$$h_{411} = -2(v_{21} + m_p\phi_{21,e})\phi_{12,e}\phi'_{11,e}$$
$$h_{412} = -2(v_{22} + m_p\phi_{22,e})\phi_{12,e}\phi'_{12,e}$$
$$h_{413} = -2(v_{21} + m_p\phi_{21,e})\phi_{12,e}\phi'_{11,e}$$
$$h_{414} = -2(v_{22} + m_p\phi_{22,e})\phi_{12,e}\phi'_{12,e}$$
$$h_{415} = -(\phi_{12,e} + \ell_1\phi'_{12,e})$$
$$h_{416} = -\phi_{12,e}$$
$$h_{417} = -(\phi_{11,e}\phi'_{12,e} + \phi_{12,e}\phi'_{11,e})$$
$$h_{418} = -2\phi_{12,e}\phi'_{12,e}$$
$$h_{419} = -(m_2d_2 + m_p\ell_2)\phi_{12,e}$$
$$h_{420} = -(v_{21} + m_p\phi_{21,e})\phi_{12,e}$$
$$h_{421} = -(v_{22} + m_p\phi_{22,e})\phi_{12,e}$$
$$h_{422} = -(m_2d_2 + m_p\ell_2)(\phi_{12,e}\phi'_{11,e} - \phi_{11,e}\phi'_{12,e})$$

$$h_{501} = (v_{21} + m_p\phi_{21,e})\ell_1$$
$$h_{502} = 2(v_{21} + m_p\phi_{21,e})\phi_{11,e}$$
$$h_{503} = 2(v_{21} + m_p\phi_{21,e})\phi_{12,e}$$
$$h_{504} = v_{21} + m_p\phi_{21,e}$$
$$h_{505} = -(v_{21} + m_p\phi_{21,e})\phi_{11,e}$$

$$h_{506} = -(v_{21} + m_p\phi_{21,e})\phi_{12,e}$$

$$h_{601} = (v_{22} + m_p\phi_{22,e})\ell_1$$
$$h_{602} = 2(v_{22} + m_p\phi_{22,e})\phi_{11,e}$$
$$h_{603} = 2(v_{22} + m_p\phi_{22,e})\phi_{12,e}$$
$$h_{604} = v_{22} + m_p\phi_{22,e}$$
$$h_{605} = -(v_{22} + m_p\phi_{22,e})\phi_{11,e}$$
$$h_{606} = -(v_{22} + m_p\phi_{22,e})\phi_{12,e}.$$

Although some of the aforementioned coefficients are equal—or related by simple factors—there is no need for reducing the total number of them, since their values are computed off-line once for all.

REFERENCES

[1] A. De Luca and B. Siciliano, "Trajectory control of a nonlinear one-link flexible arm," *Int. J. Contr.*, vol. 50, pp. 1699–1716, 1989.

[2] A. De Luca, L. Lanari, and G. Ulivi, "Output regulation of a flexible robot arm," in *Proc. 9th INRIA Int. Conf. Analysis and Optimization Syst.*, Antibes, France, June 1990, pp. 833–842.

[3] J.-J. E. Slotine and W. Li, "On the adaptive control of robot manipulators," *Int. J. Robotics Res.*, vol. 6, no. 3, pp. 49–59, 1987.

[4] E. Bayo and B. Paden, "On trajectory generation for flexible robots," *J. Robotic Syst.*, vol. 4, pp. 229–235, 1987.

[5] L. Meirovitch, *Analytical Methods in Vibrations*.. New York: Macmillan, 1967.

[6] R. H. Cannon, Jr. and E. Schmitz, "Initial experiments on the end-point control of a flexible one-link robot," *Int. J. Robotics Res.*, vol. 3, no. 3, pp. 62–75, 1984.

[7] G. G. Hastings and W. J. Book, "A linear dynamic model for flexible robotic manipulators," *IEEE Contr. Syst. Mag.*, vol. 7, no. 1, pp. 61–64, 1987.

[8] W. H. Sunada and S. Dubowsky, "The application of finite element methods to the dynamic analysis of flexible linkage systems," *ASME J. Mechanical Design*, vol. 103, pp. 643–651, 1983.

[9] P. B. Usoro, R. Nadira, and S. S. Mahil, "A finite element/Lagrangian approach to modeling lightweight flexible manipulators," *ASME J. Dynamic Syst., Measurement, Contr.*, vol. 108, pp. 198–205, 1986.

[10] S. Nicosia, P. Tomei, and A. Tornambè, "Dynamic modeling of flexible robot manipulators," in *Proc. 1986 IEEE Int. Conf. Robotics Automat.*, San Francisco, CA, Apr. 1986, pp. 365–372.

[11] F. Bellezza, L. Lanari, and G. Ulivi, "Exact modeling of the slewing flexible link," in *Proc. 1990 IEEE Int. Conf. Robotics Automat.*, Cincinnati, OH, May 1990, pp. 734–739.

[12] E. Barbieri and Ü. Özgüner, "Unconstrained and constrained mode expansions for a flexible slewing link," *ASME J. Dynamic Syst., Measurement, Contr.*, vol. 110, pp. 416–421, 1988.

[13] W. J. Book, "Recursive Lagrangian dynamics of flexible manipulator arms," *Int. J. Robotics Res.*, vol. 3, no. 3, pp. 87–101, 1984.

[14] R. P. Judd and D. R. Falkenburg, "Dynamics of nonrigid articulated robot linkages," *IEEE Trans. Automatic Contr.*, vol. AC-30, pp. 499–502, 1985.

[15] M. Benati and A. Morro, "Dynamics of chain of flexible links," *ASME J. Dynamic Syst., Measurement, Contr.*, vol. 110, pp. 410–415, 1988.

[16] S. Cetinkunt and W. J. Book, "Symbolic modeling and dynamic simulation of robotic manipulators with compliant links and joints," *Robotics & Computer-Integrated Manufacturing*, vol. 5, pp. 301–310, 1989.

[17] A. De Luca, P. Lucibello, and F. Nicolò, "Automatic symbolic modeling and nonlinear control of robots with flexible links," in *Proc. IEE Work. on Robot Control*, Oxford, UK, Apr. 1988, pp. 62–70.

[18] P. Tomei and A. Tornambè, "Approximate modeling of robots having elastic links," *IEEE Trans. Syst., Man, Cybern.*, vol. SMC-18, pp. 831–840, 1988.

[19] V. A. Abelov, "Comparisons of remote manipulator systems finite element models," The Charles Stark Draper Laboratory Inc., Rep. R–1210, 1978.

[20] P. K. Nguyen, R. Ravindran, R. Carr, D. M. Gossain, and K. H. Doetsch, "Structural flexibility of the shuttle remote manipulator system mechanical arm," SPAR Aero\-space Ltd., Tech. Info. AIAA, 1982.

[21] A. De Luca and B. Siciliano, "Dynamic modeling of multi-link flexible robot arms," in *Proc. IFIP Int. Conf. on Modeling the Innovation*, Roma, Italy, pp. 193–200, Mar. 1990.

[22] A. De Luca and B. Siciliano, "Explicit dynamic modeling of a two-link felxible manipulator," in *Proc. 29th IEEE Conf. Decision Contr.*, Honolulu, HI, Dec. 1990, pp. 528–530.

[23] C. M. Oakley and R. H. Cannon, "Initial experiments on the control of a two-link manipulator with a very flexible forearm," in *Proc. 1988 Amer. Contr. Conf.*, Atlanta, GA, June 1988. pp. 996–1002.

[24] E. Schmitz, "Modeling and control of a planar manipulator with an elastic forearm," in*Proc. 1989 IEEE Int. Conf. Robotics Automation*, Scottsdale, AZ, May 1989, pp. 267–278.

[25] C. M. Oakley and R. H. Cannon, "End-point control of a two-link manipulator with a very flexible forearm: Issues and experiments" in *Proc. 1989 Amer. Contr. Conf.*, Pittsburgh, PA, June 1989, pp. 1381–1388.

[26] C. M. Oakley and R. H. Cannon, "Equations of motion for an experimental planar two-link flexible manipulator," in *Proc. 1989 ASME Winter Annu. Meet.*, San Francisco, CA, Dec. 1989, pp. 267–278.

[27] S. Cetinkunt and W. L. Yu, "Closed loop behavior of a feedback controlled flexible beam," *Int. J. Robotics Res.*, to appear, 1990.

[28] S. Cetinkunt, B. Siciliano, and W. J. Book, "Symbolic modeling and dynamic analysis of flexible manipulators," in *Proc. 1986 IEEE Int. Conf. Syst., Man, Cybern.*, Atlanta, GA, Oct. 1986, pp. 798–803.

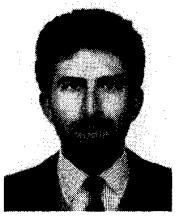

Alessandro De Luca (S'81–M'82–S'83–S'84–M'84–M'86) was born in Rome, Italy, on October 11, 1957. He received the Laurea degree in electronic engineering and the Research Doctorate degree in systems engineering, in 1982 and 1987, respectively, both from the University of Rome "La Sapienza."

Since 1983, he has been working at the Department of Computer and Systems Science, Università di Roma "La Sapienza," where he is currently a Research Associate. From Fall 1985 to Spring 1986 he was a Visiting Scholar at the Robotics and Automation Laboratory of the Rensselaer Polytechnic Institute, Troy, NY. His research interests include nonlinear control with applications to robotics, modeling and control of manipulators with elastic joints and flexible links, redundant manipulators, and hybrid force-velocity robot control.

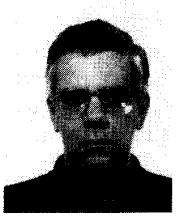

Bruno Siciliano (M'91) was born in Naples, Italy, on October 27, 1959. He received the Laurea and the Research Doctorate degrees in electronic engineering, both from the University of Naples in 1982 and 1987, respectively.

Since 1983 he has been working at the Department of Computer and Systems Science, Università di Napoli "Federico II," Naples, Italy, where he is currently a Research Associate. From Fall 1985 to Spring 1986 he was a Visiting Scholar at the School of Mechanical Engineering of the Georgia Institute of Technology, Atlanta, GA, under a NATO research fellowship. He is a Technical Editor of the IEEE TRANSACTIONS ON ROBOTICS AND AUTOMATION. His research interests include manipulator inverse kinematics techniques, modeling and control of lightweight flexible arms, redundant manipulator control, cooperative robot manipulation, and output feedback control of two-time scale systems.